Avrupa Bilim ve Teknoloji Dergisi
Özel Sayı 32, S. 92-100, Aralık 2021

Araştırma Makalesi

www.ejosat.com ISSN:2148-2683

European Journal of Science and Technology
Special Issue 32, pp. 92-100, December 2021

Research Article

Acquiring Kinematics of Lower extremity with Kinect

İrfan Kösesoy[1*], Cemil Öz[2]

[1*] Kocaeli University, Faculty of Engineering, Departmant of Software Engineering, Kocaeli, Turkey, (ORCID: 0000-0001-5219-5397), irfan.kosesoy@kocaeli.edu.tr
[2] Sakarya University, Faculty of Computer and Information Sciences, Departmant of Software Engineering, Sakarya, Turkey, (ORCID: 0000-0001-9742-6021), coz@sakarya.edu.tr

(International Conference on Design, Research and Development- 20 – 22 October 2021)

(**DOI:** 10.31590/ejosat.1041675)

ATIF/REFERENCE: Kösesoy, İ. & Öz, C. (2021). Acquiring Kinematics of Lower extremity with Kinect. *European Journal of Science and Technology*, (32), 92-100.

Abstract

Gait analysis is used in monitoring the procedures of treatment and determining many illnesses notably musculoskeletal system disorders. Gait analysis has been carried out with divergent methods for a long time. In this study, kinematic parameters of lower human extremities are determined using Kinect, a camera called Time of Flight that is usually used in the entertainment sector. Kinect is recommended as a low-cost solution for existing gait analysis systems. Kinematic parameters that are used to analyze walking are found by filtering RGB images of colored markers that are attached to joints. 3D world coordinates of the marker centers were determined and labeled by mapping the depth information, which is obtained from Kinect, on RGB images. We used the Kalman filter to estimate the coordinates of markers when the coordinates cannot be accurately determined because of motion blurring. 15 kinematic parameters for each joint are extracted from the coordinates of these markers.

Keywords: Human Motion Analysis, Microsoft Kinect, Kinematics, Gait.

Kinect Kullanarak Alt Ekstremiteye Ait Kinematiğin Elde Edilmesi

Öz

Yürüyüş analizi, tedavi süreçlerinin izlenmesinde ve başta kas-iskelet sistemi rahatsızlıkları olmak üzere birçok hastalığın belirlenmesinde farklı teknikler kullanılarak yapılmaktadır. Bu çalışmada, genellikle eğlence sektöründe kullanılan Time of Flight adlı bir kamera olan Kinect kullanılarak alt insan ekstremitelerinin kinematik parametreleri belirlendi. Çalışmada önerilen sistem, mevcut yürüyüş analiz sistemleri için düşük maliyetli bir çözüm olarak önerildi. Yürümeyi analiz etmek için kullanılan kinematik parametreler, eklemlere eklenen renkli işaretçilerin RGB görüntülerini filtreleyerek bulundu. Kinect'ten elde edilen derinlik bilgisi RGB görüntüler üzerine haritalanarak işaretleyici merkezlerinin üç boyutlu dünya koordinatları belirlenmiş ve etiketlenmiştir. Hareket bulanıklığı nedeniyle koordinatların tam olarak belirlenemediği işaretçilerin konumları Kalman filtresi ile tahmin edildi. Her eklem için 15 kinetik parametre bu işaretçilerin koordinat bilgileri kullanılarak çıkarıldı.

Anahtar Kelimeler: Yürüme Analizi, Microsoft Kinect, Yürüme Kinematiği.

[*] Corresponding Author: irfan.kosesoy@kocaeli.edu.tr

1. Introduction

Gait Analysis is a systematic study carried out by measuring the motion and activities during walking and takes advantage of technologic utilities[1]. Human eye cannot perceive events faster than 1/12 second and cannot follow motions happening at the same time on different planes. Therefore, gait cannot be evaluated with human eye as it is a complex process[2]. In order to have an objective evaluation carried out by the professionals in the same field, techniques where it is possible to evaluate walking qualitatively and quantitatively have been developed. Kinetics, kinematics and electromyographic measures regarding walking are performed with these methods[3]. Kinetics is the pressure applied to the ground by the foot during the walking and measurements are taken by force plates or force shoes. Electromyography is the process of measuring the electrical activity in the muscles with sensors placed on the body. Kinematics recommended to be found with Kinect is the measurements regarding the motion of the segments. Publications where the development processes of electromyographic, kinematics and kinetics measurements in clinical gait analysis are elaborately explained by Sutherland [4]–[6].

Human motion tracking systems are used in retrieving the kinematics. Motion tracking systems are classified as Visual tracking, Non-visual tracking and Robot aided tracking in [7]. Systems such as VICON, Optortrack, Qualysis used in gait analysis most often and acknowledged as gold standard in motion tracking are marker based visual motion tracking systems. Passive markers are used in these systems. Infrared lights expanding in the environment hits these markers and perceived by the cameras. System calculates the 3D coordinates of these markers and then combines them with 2D images gathered by the cameras[7], [8].

Even though systems such as Vicon and Qualysis gives the human kinematics with high accuracy, their high costs, hard set up and difficult use lead the researchers to develop low-cost and easy-to-use alternatives in motion tracking[9]. To that end, studies have been carried out on the use of depth cameras similar to Kinect in gathering 3D data in motion tracking. Kinect provides depth and RGB images. It also gives the skeletal data of the people.

Markerless visual gait tracking is an active research area. The increase in the number of cameras in these systems also increases the accuracy but also complicates the setup and the calibration of the system. The most important data in 3D gait analysis is gathered via sagittal plane. However, due to the fact that the body is not parallel to the depth sensor or obstacles caused by orientation during walking, skeletal data is not highly accurate.

As the skeletal data that Kinect provides without using markers doesn't lead to satisfying results in the studies conducted in this area, researchers resort to using different systems with skeletal data or making pose estimation from the depth data [9]–[12]. In [9], skeletal data gathered fusing more than one kinect's data as well as wearable inertial sensors is used to retrieve kinematics. In [10], [11], pose estimation is made by observing the segmented body in the depth map. One of the important problems of these systems is that gathering 3D location data requires intense calculation.

In this study, the objective is to develope a low cost system that can be used in retrieving kinematics regarding lower extremity. In the proposed system, the segment locations and joint angles are determined with the help of the colored markers. Markers are filtered via RGB images and the central coordinates of the markers are extracted. To find depths of these coordinates, RGB images are mapped on to depth images. Using the depth data and image coordinates, 3D coordinate data are gathered.

The remainder of this paper is organized as follows. In chapter two, system modules are explained briefly. The software and hardware technologies are introduced and scanning geometry of Kinect was explained. In chapter three, marker layout and how the gathered kinematics are briefly explained. In chapter four, gathering and processing data, in chapter 5, blurring problem and its solution, and finally in chapter 6, registration results are shown.

2. System Overview

System is composed of five modules as it can be seen on Figure 1. In order to retrieve accurate data, recording environment is prepared to be as quiet as possible. To prevent noise while filtering the markers, it is very important that neither the background nor the clothes of people do not contain the same color as the markers. As the record taken from the sagittal plane, Kinect placed parallel to the walking path. Distance between the Kinect and walking path is determined in a way to minimize the measuring mistakes in the depth component of the data. Kinect can detect a depth of around 13.1 feet (4.0 meters). In addition, the depth of objects closer than 40 cm cannot be detected. As the distance between walking path and Kinect increases, sight will increase and a longer field will be recorded. However when the depth limit of the Kinect and the accuracy of the filtering the markers are taken into consideration, 3 meters distance is determined to be adequate.

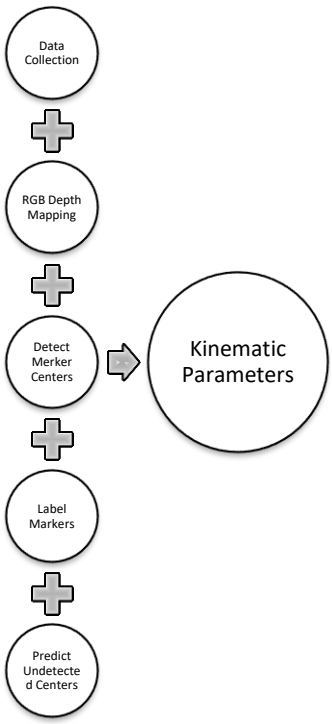

Fig. 1. Block diagram of the system

2.1. System Hardware

Kinect, a time of flight camera, is used to collect data. Kinect sensor that was developed in 2010 for Xbox 360 game console is a device with color camera and 3 microphones[14](Figure 2).

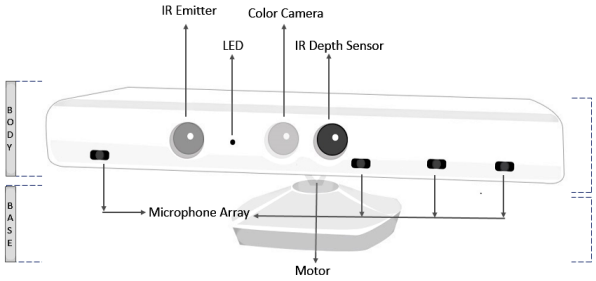

Fig. 2. Kinect Device

It has 640x480 pixel resolution and can take RGB and depth maps at the speed of 30 fps. Kinect has a viewpoint of 47 degrees vertically and 57 degrees horizontally. Having a motor, it can move 27 degrees up and down on the vertical axis.

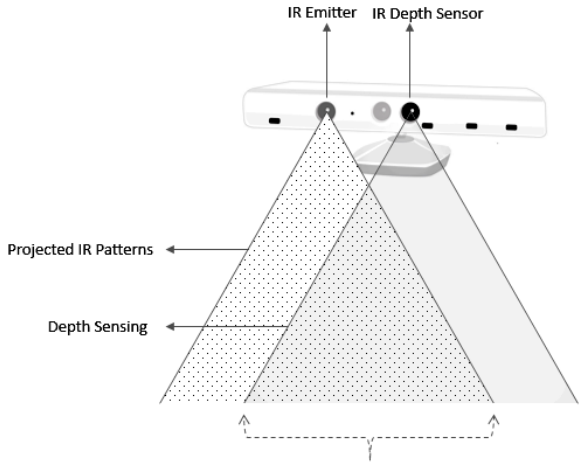

Fig. 3. Kinect depth sensing

Kinect perceives depth with infrared (IR) emitter and IR depth sensors. IR emitter and infrared light spreads and these rays reflected after hitting objects are detected by IR depth sensors and converted into depth info. As the area where IR emitter sends out light and IR depth sensor detects the rays are different, so the area of which depth was detected in the viewpoint is smaller(figure 3) [13]. For this reason, RGB and depth images taken simultaneously and at the same resolution does not match. To find the depth of a point on the RGB image, depth data should be mapped onto the color image. In this study, after finding the marker centers on colored image, depth of the center was found by making RGB/Depth mapping.

After Kinect was released, it started to be used in many projects. One of the most important reasons why it became that successful is that it finds and track the skeleton of the people during the study. Kinect detects 20 points of the human body and gathers their image and world coordinates. When the skeletal data are drawn on image, it was observed that the skeleton lapses on many frames. Therefore, if the skeletal data gathered by just one Kinect may lead to serious mistakes on gait kinematics. In this study in order to get more accurate data, colored markers are used instead of the skeleton which provided byKinect

Data are gathered by a Kinect connected to a pc with 8 GB Ram and 2.4 GHz processor. Microsoft SDK was used for the records. After gathering the data; filtering, detecting the centers, labeling the markers, estimating the missing centers, finding the kinematic parameters and visual output processes have been carried out on Matlab.

2.2. Camera Calibration

Calibration is a transformation made between 3D coordinate planes and 2D image planes with the knowledge of the camera's intrinsic parameters[15]. The relation between a point in 3D at position(X,Y,Z) and its image (x,y) on a camera specified in pixel coordinates are demonstrated in figure 5.

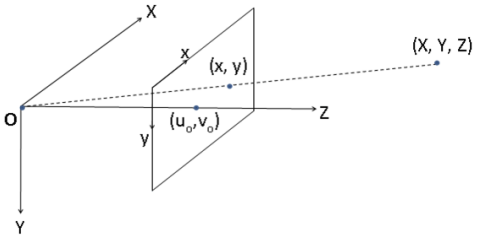

Fig. 4 Projection of a point in 3D on camera specified pixel coordinates

Hence the figure, Z axis is right to the image and intersects with the image plane on the principal point (u0, v0). For the translation the 3D coordinates into pixels the 2D image position must be divided by, respectively, the pixel width(px) and height(py). The focal length given in world units is dividing by px, the obtained focal length expressed in pixels and defined as fx. Similarly fy = f/py is defined as focal length expressed in vertical pixel unit. While determining the locations where the points gathered from real world will be located, principal point which passes through focal point and where the image intersects with the axis is taken as a base. After knowing the principal point (u0,v0) and focal length (fx,fy) of a digital camera, a point in the 3D space (X,Y,Z) is transferred to the 2D plane by using equation 1-2[16].

$$x = \frac{f_x X}{Z} + u_0 \qquad (1)$$

$$y = \frac{f_y Y}{Z} + v_0 \qquad (2)$$

These equations can be rewritten in matrix form through the introduction of homogeneous coordinates. Here is the projective equation rewritten.

$$\begin{bmatrix} x \\ y \\ 1 \end{bmatrix} = \begin{bmatrix} f_x & 0 & u_0 \\ 0 & f_y & v_0 \\ 0 & 0 & 0 \end{bmatrix} \begin{bmatrix} 1 & 0 & 0 & 0 \\ 0 & 1 & 0 & 0 \\ 0 & 0 & 1 & 0 \end{bmatrix} \begin{bmatrix} X \\ Y \\ Z \\ 1 \end{bmatrix} \qquad (3)$$

Intrinsic parameters of the sensors are given by manufacturers. However, in the studies requiring more sensitive

results, the intrinsic and extrinsic parameters are usually determined by using a chessboard.

In this study, it was tried to acquire world coordinates of marker center by the image coordinates, namely doing the opposite of what has been said above. In case of knowing the depth (Z) of a point in real world, (X,Y) coordinates can be achieved as in equation 4 and 5 by applying inverse transformation to the equations 1 and 2.

$$X = \frac{(x-u_0)Z}{f_x} \quad (4)$$

$$Y = \frac{(y-v_0)Z}{f_y} \quad (5)$$

3. The Human Kinematic

In most textbooks on anatomy the primary planes of the human body are defines as in the figure 5 [1]. During the process of walking, the body moves on the sagittal, frontal and transverse planes. In 3D gait analysis, all motions on all planes can be detected. Many motions during walking happen on sagittal plane. Hence amongst these 3 planes, motions on the sagittal plane contains the most important data[17].

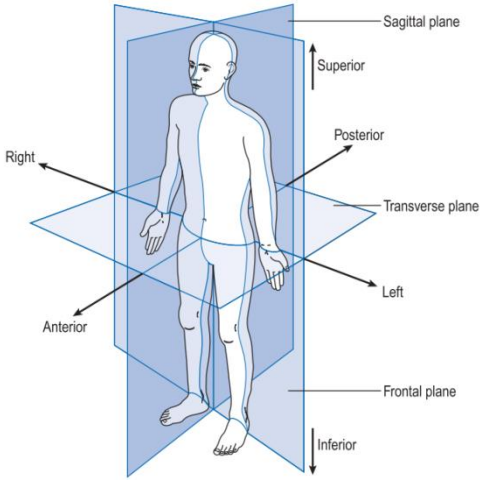

Fig. 5 The anatomical position, with three reference planes and six fundamental directions. Figure from [18]

Kinematics are used to define the movements of limb segment and joints. Two kinds of motion is observed during walking that are angular and linear. Kinematic parameters are the data of angular and linear substitution, velocity and acceleration of the joints and limb segments[2]

Several spatial systems have been proposed. The one utilized throughout the study is the one often used for human gait. It was decided that the direction of progression(anterior-posterior) is X, vertical direction is Y and the distance between the walking path and Kinect is Z. Angles are on the XY and YZ planes and increases positively on clockwise.

The complete kinematics of any body segment requires 15 data variables, all of which are changing with time [19]. These variables are defines as follows

- Position (x, y, z) of segment center of mass
- Linear velocity ($\dot{x}$,$\dot{y}$,$\dot{z}$) of segment center of mass
- Linear acceleration ($\ddot{x}$,$\ddot{y}$,$\ddot{z}$) of segment center of mass

As RGB images and Depth data are gathered by different sensors, the images don't match completely even when their resolutions are equal. Depth map has a smaller sight when compared to the RGB image. Therefore a calibration between sensors is required to find the depth of the marker centers via RGB image.

While it is possible to find the RGB coordinates via depth coordinates with Microsoft Kinect SDK, there is no method to carry out the opposite. In the study, color codes equal to depth coordinates for each frame were determined then depth coordinates of color coordinates found by applying inverse transformation.

- Angle of segment in two planes, θxy, θyz
- Angular velocity of segment in two planes, ωxy, ωyz
- Angular acceleration of segment in two planes, αxy, αyz

3.1. Limb-Segment Angles

The colored markers are placed as it is shown in figure-6 to find the kinematics parameters. To be able to find the limb angles, it is not necessary that the two markers be at the extreme ends of the limb segment, as long as they are in line with the long-bone axis [19].

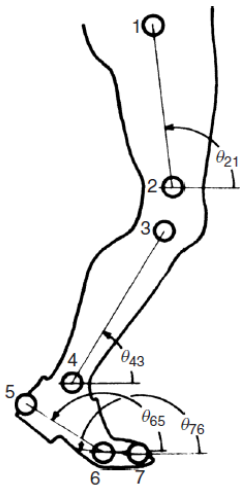

Fig. 6 Marker location and limb and joint angles using an established convention. Figure from [19]

In Figure 6, placement of the markers used to calculate the kinematics is shown. Markers 1 and 2 define the thigh in the sagittal plane. By convention all angles are measured in counterclockwise direction, starting with the horizontal equal to 0º. Thus, θ 21 is the angle of the thigh in space and can be calculated according to equation- 6.

$$\theta_{ij} = tan^{-1}\left(\frac{y_j-y_i}{x_j-x_i}\right) \quad (6)$$

According to this placement, clockwise motion is decided to be positive for the velocity, acceleration and angle values. There are six different angles in total. These angles:

Angle	Limb - Segment

θ_{21}	*Thigh angle*
θ_{43}	*Shank angle*
θ_{65}	*Foot angle*
θ_{76}	*Metatarsal*
$\theta_{knee} = \theta_{21} - \theta_{43}$	*Knee (+ for flexion and – for extension)*
$\theta_{ankle} = \theta_{43} - \theta_{65} + 90$	*Ankle (+ for plantar flexion and – for dorsi flexion)*

Table 1. Limb-segment angle notation

The segment angles that are acquired according to the planes taken as reference are the absolute angles. The absolute angles can be found by using two consecutive marker centers. It is quite easy to calculate the joint angles from the angles of the two adjacent segments. For example when finding the knee angle, thigh and shank angles are used. There is a convention for describing the magnitude and polarity of each joint. For example when the knee is fully extended, it is described as 0º flexion. As it is seen on the equation 7, when θ21 is bigger than θ43, the result is positive and the knee is flexed otherwise the knee is extended.

$$\theta_{knee} = \theta_{21} - \theta_{43} \quad (7)$$

$$\theta_{ankle} = \theta_{43} - \theta_{65} + 90 \quad (8)$$

The ankle angle seen on equation 8 is also a relative angle. However, different than the knee, as the angle between shank and foot is 90º, the angle between is found by adding 90º to the difference between the foot and shank absolute angles. If θankle is positive, the foot is plantarflexed; if θankle is negative, the foot is dorsiflexed.

3.2. Velocities and Accelerations

There are two kinds of motion that are observed in the body during walking - linear and angular. With the linear motion , there is also an angular motion depending on the rotations in the joints at the same time. The velocity and acceleration parameters are found linearly and angularly by 3D marker centers.

The velocity of the displacement data is Δx/Δt where Δt and Δx are the passed time and the displacement between two adjacent samples. The velocity calculated this way does not represent the velocity of a point in time halfway between two samples. I represent velocity of a point in time halfway between two samples (figure 7). A way around this problem is to calculate the velocity and acceleration in the basis of 2Δt rather then Δt [19]. Thus as it is seen on Fig.7, velocity at the x moment is :

$$V_i = \frac{x_{i+1} - x_{i-1}}{2\Delta t} \quad (9)$$

Linear velocity is found on the equation 9. Likewise, if the angle values are used in the equation instead of the displacement, then the angular velocity equation is :

$$\Omega_i = \frac{\theta_{i+1} - \theta_{i-1}}{2\Delta t} \text{ rad/s} \quad (10)$$

After finding the velocity, the acceleration can also be found as following by taking the velocity values as the basis.

$$\alpha_i = \frac{v_{i+1} - v_{i-1}}{2\Delta t} \text{ m/s}^2 \quad (11)$$

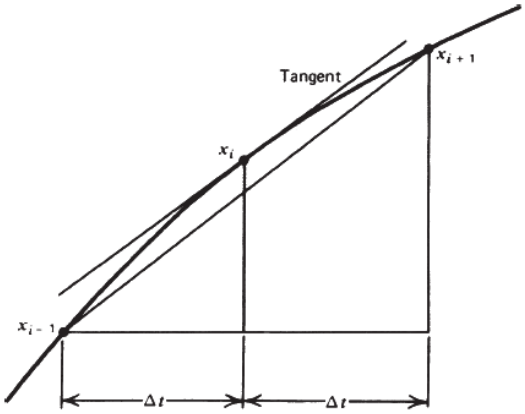

Fig. 7 Finite-difference technique for calculating the slope of a curve at the i th sample point. Figure from [19]

According to the equation 11 the acceleration parameter requires displacement data from samples I+2 and I-2, thus a total of five successive data points go into the acceleration. An alternative and slightly better calculation of acceleration uses only three successive data coordinates and utilizes the calculated velocities halfway between sample times :

$$V_{i+1/2} = \frac{x_{i+1} - x_i}{\Delta t} \quad (12.a)$$

$$V_{i-1/2} = \frac{x_i - x_{i-1}}{\Delta t} \quad (12.b)$$

If these found values are put into place in equation 11, the linear acceleration finally becomes as in the equation 12.c.

$$\alpha_i = \frac{x_{i+1} - 2x_i + x_i}{\Delta t^2} \text{ m/s}^2 \quad (12.c)$$

In linear acceleration equations, the angular acceleration also can be similarly calculated by using the angular velocity instead of the location data.

4. Data Collection and Processing

Before gathering the data, the recording environment is prepared as mentioned in chapter 2. The RGB and Depth data are acquired in the resolution of 640x480 pixels and as 30 fps. To detect the depth of the marker centers' that will be filtered via RGB image, it is mapped onto depth data. To prevent the markers from slipping during walking, the tight clothes are supposed to be worn.

4.1. Marker Segmentation

Image segmentation is the process of dividing the homogeneous areas on the image from each other. This process is the first and most important step of image analysis and pattern recognition. There are many studies in the literature on segmentation of the monochrome and color images. Though colored images contains more information than the monochrome images, process complication is much more in colored images because of evaluating more than one band in segmentation[20]. Recently, with the increase in performance of personal computers, studies on colored image segmentation has also increased.

In color image segmentation, RGB images are converted into different color spaces such as HSV, YCrCb, TSL and the problems caused by high correlation between RGB bands are tried to be overcome. As the records will be taken in a controlled environment and only red areas will be filtered in this study, segmentation is conducted in RGB color space.

After converting the RGB image into gray, it is extracted from R component and filtered with median filter, than a proper threshold value is detected. The image is converted into binary image according to the threshold value. Lastly, the acquired binary image undergoes blob analyze and the image coordinates of filtered red regions and surface area are determined. Determined areas are sorted based on their surface areas and the areas where no markers were thought to be there are eliminated. The image coordinates of seven points are acquired from the filtered image. In some images, the centers might be less than seven due to the blur effect happened to markers during walking.

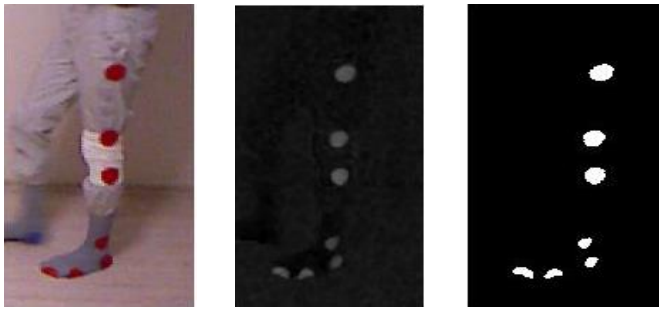

a b c

fig. 8 a) Kinect RGB image b) Extracted gray-scale image c) Filtered binary image.

4.2. Marker Labeling

The centers found after the markers were segmented are labeled from 1 to 7. While labeling the markers, changes in the x and y coordinates caused by rotation in the feet during walking are taken into consideration. When the degree of freedom of each marker is taken into account, groups are composed amongst markers where gradation doesn't change. For the labeling, all markers need to be determined. After all marker centers (7 points) are found, labeling takes place in three stages. In the first stage, the determined coordinates are aligned according to the y value. As the first three markers aligned starting from the upper leg doesn't change in terms of y coordinate alignment and their y value is smaller than the y value of the markers on the areas of lower leg and feet, the first three markers are labeled in the first phase. The regions seen on the Figure 9 are labeled as 1, 2, and 3 consecutively according to their increasing y values. In the second stage, the unlabeled four markers are aligned according to the x coordinate. In the alignment made, when the Region-2 markers in the Fig. 9 are aligned according to decreasing x coordinate, they are labeled as 7 and 6 consecutively. In the last stage, the remaining two markers are again aligned according to the y coordinate values and are labeled as 4 and 5 according to the increasing value (fig. 9 Region-3)

Steps used in the labeling are as follows:

1. Align the determined centers according to increasing y values.
2. Label the first 3 centers consecutively as 1, 2, and 3.
3. Align the unlabeled centers according to x values.
4. Appoint the labels 6 and 7 to the first two centers.
5. Align the unlabeled centers according to y values.
6. Appoint the labels 4 and 5 to the first two centers.

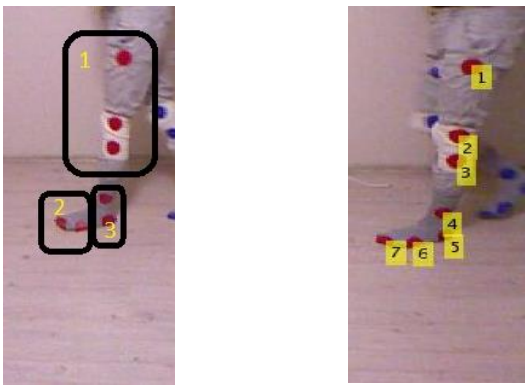

a b

Fig. 9 a) markers sorted before labeling b) labeled sample image.

4.3. Blurring Problem

The most crucial problem encountered while collecting and processing data is the blur effect happening in the markers in swing phase. In Fig. 9-.a the regions numbered 2 and 3 are blurred in the moment when the foot accelerates. Especially the markers in the region -2 are either cannot be detected or the red areas merged because of the blurring. (fig 10). In this case, due to the absence of the centers, the labeling algorithm proposed in the chapter 4.2 gives errors. To deal with that problem, the missing marker centers are detected by comparing the frames where the markers are complete and where the markers are incomplete. The frames with n(n<7) marker centers are compared to the previous frames where the centers have been complete and by taking their distance to each other according to the x and y axes as the basis, the matching possibility of the markers are detected.

$$P_x(i,j) = 1 - \frac{[\![rx_i - x_j]\!]}{\sum_{i=1}^{7}\sum_{j=1}^{n}[\![rx_i - x_j]\!]} \quad (13)$$

$$P_y(i,j) = 1 - \frac{[\![ry_i - y_j]\!]}{\sum_{i=1}^{7}\sum_{j=1}^{n}[\![ry_i - y_j]\!]} \quad (14)$$

Px and Py are matrixes at the size of 7xn in the equations 13 and 14 - they express the conjugation possibility of the markers. By looking at the possibility matrixes, each one of the n markers gets the same label as the marker whose possibility is the greatest for it. The locations of the markers that cannot be detected are estimated by Kalman filter.

Fig. 10 A sample image where blur can be observed

4.3.1. Kalman Filter

Kalman filter is a sequence of some mathematical equations that estimates the status of the system recursively. It takes the previous outputs and estimation values of a dynamic system into account and uses them to estimate the new case and updates its estimations according to new inputs [21] [22]. It was proposed by R.E. Kalman[23] in 1960 and started to be used in different fields since then. One of the fields where Kalman filter is frequently used is

object tracking. It is used in the frames where the object that is being tracked bumps into an obstacle or it cannot be detected to estimate the status of the object[22], [24]–[27],[28].

The purpose in the tracking system is to estimate the location of the object in discrete time by using the xk state vector and zk measurement method where the object is kept.

$$x_k = Ax_{k-1} + w_{k-1} \quad (15)$$

$$z_k = Hx_k + v_k \quad (16)$$

The equation 15 shows the transition of xk state vector from k-1 to k state. A is transition matrix here and wk-1 is the process noise. In the equation 16, H is the measurement matrix and zk is the measurement in the transition from k-1 discrete time to k. vk is the measurement noise mentioned as Gaussian.

In the equation 15 and 16 when the measurement equation are written consecutively, the recursive processes are composed of the time update (prediction) and the measurement update (correction) phases.

$$\grave{x}_k^- = A\grave{x}_{k-1} + w_k \quad (17)$$

$$\grave{P}_k^- = AP_{k-1}A^T + Q \quad (18)$$

In the time update phase x`_k^- is the raw estimation of the previous case. Likewise P`_k^- is the previous error covariance. These detected values are used as prior values in the measurement update phase.

$$K_k = \grave{P}_k^- H^T (H\grave{P}_k^- H^T + R)^{-1} \quad (19)$$

$$K_k = \grave{P}_k^- H^T (H\grave{P}_k^- H^T + R)^{-1} \quad (20)$$

$$K_k = \grave{P}_k^- H^T (H\grave{P}_k^- H^T + R)^{-1} \quad (21)$$

It is aimed to make an aposteriori prediction for x`_k with the combination of these state vector (x`_k^-) counted as apriori in the measurement update phase and the new measurement(zk). Kalman gain (Kk) used to make aposteriori prediction is present in the equation 19. In equation 20, the error covariance(Pk) that will be used in the prediction in the next iteration is calculated.

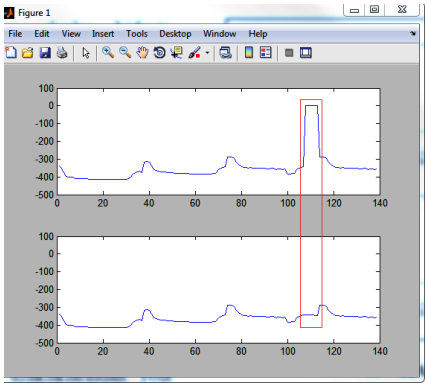

Fig. 11 Filtered y value of the marker data

Kalman filter is used to estimate the marker centers that cannot be detected due to the blurring problem during walking. In the upper graphic in Fig.11, y value of the marker-7 is drawn. 0 value in the graphic is appointed as default because no marker could be found on these frames. In the lower graphic, the estimated values produced by Kalman filter is used instead of the missing values.

5. Results

The records are collected on a 6 meters walking path from people whose kinematic will be extracted. Linear and angular motions are detected using the x, y, z coordinates of the 7 markers. While evaluating the linear motions of the limbs, the gravity centers of the markers are taken into account. The angular motions are evaluated on XY and YZ planes. Not only the absolute angles of the four limbs but also the relative angles of knee and ankle are also detected. As it is mentioned in chapter 3, 15 kinematic parameters are detected for each limb. Therefore, 60 (4x15) parameters are found in a record for all segments. The angle, the velocity and the angular acceleration parameters created relatively apart from the segments are also detected. Along with these parameters, 66 (4x15+3x2) parameters in total are found in a record.

A gait cycle is start with initial contact of foot and ends with the next time when the same foot touches the ground again.

The graphics of the detected kinematic parameters are drawn for only one gait cycle and its percentage of the period is given on the x axis. The angular parameters were divided as XY and YZ planes. The results detected for these planes are given in Fig. 12 and 13 respectively. The parameters of linear motions are drawn separately for each segment and the results are given in Fig. 14-17.

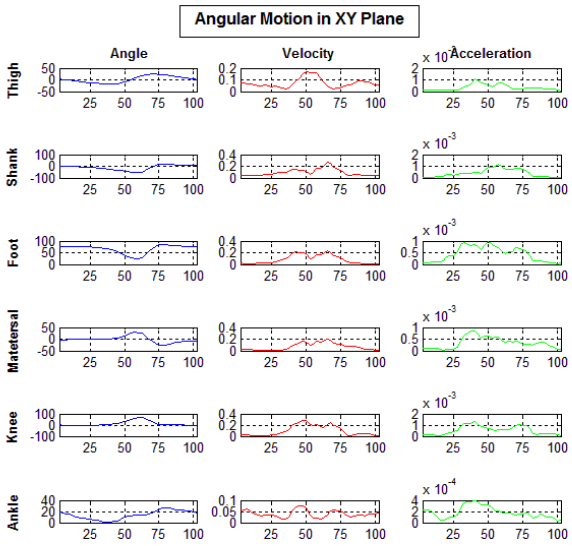

Fig. 12 Angular motion in XY Plane

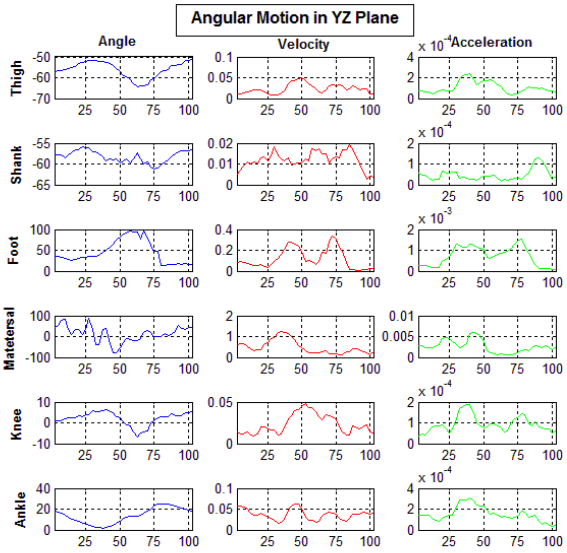

Fig. 13 Angular motion in YZ plane

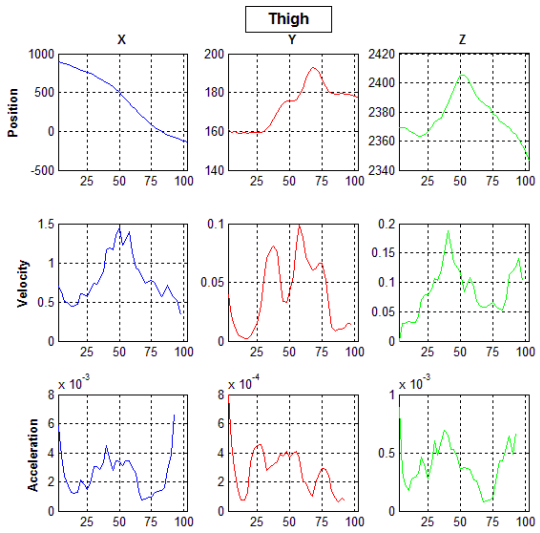

Fig. 14 Thigh linear motion

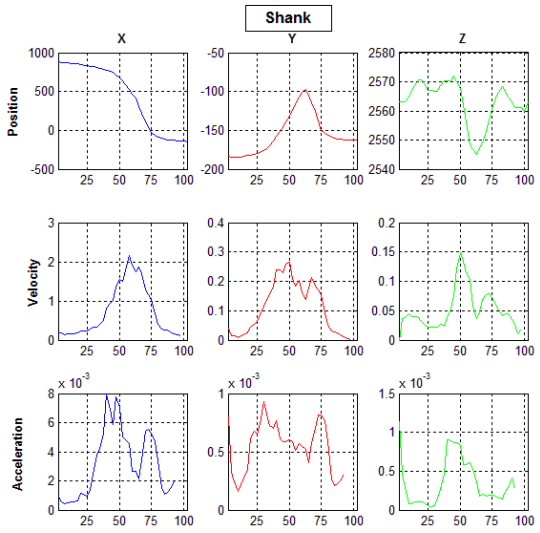

Fig. 15 Shank linear motion

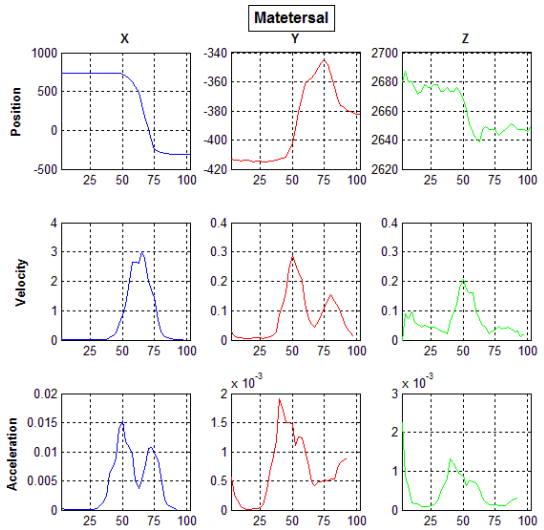

Fig. 16 Matetersal linear motion

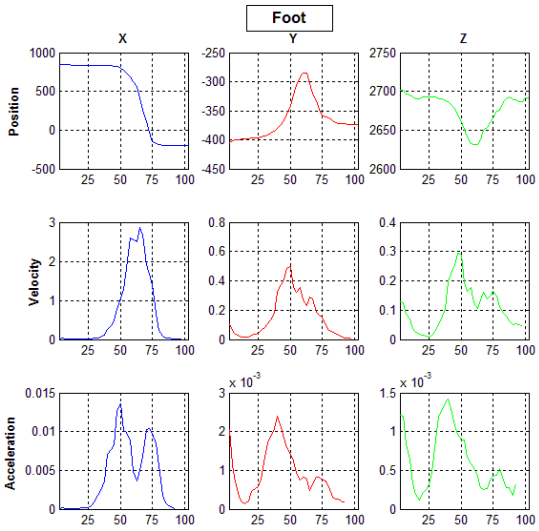

Fig. 17 Foot linear motion

The distance and time differences between the gait cycles in a record will change the graphic. Therefore, these differences are accepted to be errors for kinematic parameters. In table 2, the distance between the gravity centers of the segments in first and the last frames of each gait cycle and the mean and standard deviation values of these measurements are detected. Also in table 3, the standard deviation for time between gait cycles is given.

Stride Leng. Err.	**Mean [cm]**	**Std[cm]**
Thigh	*1.0032*	*0.6790*
Shank	*1.0003*	*0.3365*
Foot	*1.0173*	*0.4085*
Matetersal	*1.01068*	*0.4687*

Table 2. Standard deviation of stride length error

	Std
Stride Dur. Err. [sec.]	*0.1743*

Table 3. Standard deviation of stride duration error

6. Conclusion

In this study, a novel, Kinect-based, low-cost and easy-to-use system is proposed instead of the high-cost, hard to operate and also expensive systems such as Vicon and Qualysis which are used in gait analysis. Kinematic parameters of lower human extremities are extracted from the data obtained from sagittal plane using Kinect to be used in gait analysis. Kinect sensor gives lower quality results in motion tracking when compared to expensive optical tracking systems because it records with lower fps. As the image resolution and fps features of RGBD cameras advances, accuracy of the system parameters will also increase. Kalman filter is used to enhance the accuracy of the system. In this study, the acquired results are enough to carry out the gait analysis accurately and properly and they support the studies in the literature.

References

[1] M. W. Whittle, *Gait analysis: an introduction*, vol. 3. 2002.

[2] G. Yavuzer, "Three-dimensional quantitative gait analysis," *Acta Orthop. Traumatol. Turc.*, vol. 43, no. 2, pp. 94–101, 2009.

[3] M. Whittle, "Clinical gait analysis: A review," *Hum. Mov. Sci.*, vol. 15, pp. 369–387, 1996.

[4] D. H. Sutherland, "The evolution of clinical gait analysis part 1: Kinesiological EMG," *Gait and Posture*, vol. 14. pp. 61–70, 2001.

[5] D. H. Sutherland, "The evolution of clinical gait analysis: Part II kinematics," *Gait Posture*, vol. 16, pp. 159–179, 2002.

[6] D. H. Sutherland, "The evolution of clinical gait analysis part III--kinetics and energy assessment.," *Gait Posture*, vol. 21, pp. 447–461, 2005.

[7] H. Zhou and H. Hu, "Human motion tracking for rehabilitation—A survey," *Biomed. Signal Process. Control*, vol. 3, no. 1, pp. 1–18, Jan. 2008.

[8] S. E. M. L. R. G. Morris, R. Morris, and S. Lawson, "A review and evaluation of available gait analysis technologies, and their potential for the measurement of impact transmission," *Newcastle Univ.*, 2010.

[9] F. Destelle, A. Ahmadi, N. E. O'Connor, K. Moran, A. Chatzitofis, D. Zarpalas, and P. Daras, "Low-cost accurate skeleton tracking based on fusion of kinect and wearable inertial sensors." pp. 371–375, 2014.

[10] E. Stone and M. Skubic, "Evaluation of an Inexpensive Depth Camera for Passive In-Home Fall Risk Assessment," *Proc. 5th Int. ICST Conf. Pervasive Comput. Technol. Healthc.*, 2011.

[11] E. E. Stone and M. Skubic, "Passive in-home measurement of stride-to-stride gait variability comparing vision and Kinect sensing.," *Conf. Proc. IEEE Eng. Med. Biol. Soc.*, vol. 2011, pp. 6491–4, Jan. 2011.

[12] M. Gabel, R. Gilad-Bachrach, E. Renshaw, and A. Schuster, "Full body gait analysis with Kinect.," *Conf. Proc. IEEE Eng. Med. Biol. Soc.*, vol. 2012, pp. 1964–7, 2012.

[13] Microsoft Research, "Kinect for Windows SDK beta," *Program. Guid.*, pp. 1–33, 2011.

[14] Z. Zhang, "Microsoft Kinect Sensor and Its Effect," *IEEE Multimedia*, vol. 19. pp. 4–10, 2012.

[15] J. Heikkilä and O. Silvén, "A Four-step Camera Calibration Procedure with Implicit Image Correction."

[16] R. Laganière, *OpenCV 2 Computer Vision Application Programming Cookbook*. 2011.

[17] C. L. Vaughan, B. L. Davis, L. Christopher, and J. C. O. Connor, *Dynamics of human gait*, vol. 26. 2005.

[18] M. W. Whittle, *Gait analysis: an introduction*, vol. 3. 2002.

[19] D. A. Winter, *Biomechanics and motor control of human movement, Fourth Edition*, vol. 2. 2009.

[20] H. D. Cheng, X. H. Jiang, Y. Sun, and J. Wang, "Color image segmentation: Advances and prospects," *Pattern Recognit.*, vol. 34, no. 12, pp. 2259–2281, 2001.

[21] G. Welch and G. Bishop, "An Introduction to the Kalman Filter," *In Pract.*, vol. 7, pp. 1–16, 2006.

[22] S. S. Pathan, A. Al-Hamadi, and B. Michaelis, "Intelligent feature-guided multi-object tracking using Kalman filter," in *2009 2nd International Conference on Computer, Control and Communication*, 2009, pp. 1–6.

[23] R. E. Kalman, "A New Approach to Linear Filtering and Prediction Problems," *Trans. ASME-Journal Basic Eng.*, vol. 82, no. Series D, pp. 35–45, 1960.

[24] E. Cuevas, D. Zaldivar, and R. Rojas, "Kalman filter for vision tracking," *Measurement*, no. August, pp. 1–18, 2005.

[25] S. Park, S. Yu, J. Kim, S. Kim, and S. Lee, "3D hand tracking using Kalman filter in depth space," *EURASIP J. Adv. Signal Process.*, vol. 2012, no. 1, p. 36, Feb. 2012.

[26] S.-K. Weng, C.-M. Kuo, and S.-K. Tu, "Video object tracking using adaptive Kalman filter," *Journal of Visual Communication and Image Representation*, vol. 17, no. 6. pp. 1190–1208, 2006.

[27] X. Li, K. Wang, W. Wang, and Y. Li, "A multiple object tracking method using Kalman filter," *Inf. Autom. ...*, vol. 1, no. 1, pp. 1862–1866, 2010.

[28] C. Oz and M. A. L. I. Oz, "Developing and establishing a natural user interface based on Kinect sensor with artificial neural network," *Optoelectron. Adv. Mater. Commun.*, vol. 8, no. 11, pp. 1176–1186, 2014.